Science of the Total Environment 520 (2015) 187–197

Contents lists available at ScienceDirect

Science of the Total Environment

journal homepage: www.elsevier.com/locate/scitotenv

Apportioning sources of organic matter in streambed sediments: An integrated molecular and compound-specific stable isotope approach

Richard J. Cooper [a,*], Nikolai Pedentchouk [a], Kevin M. Hiscock [a], Paul Disdle [a], Tobias Krueger [b], Barry G. Rawlins [c]

[a] School of Environmental Sciences, University of East Anglia, Norwich Research Park, Norwich NR4 7TJ, UK
[b] IRI THESys, Humboldt University, 10099 Berlin, Germany
[c] British Geological Survey, Keyworth, Nottingham NG12 5GG, UK

HIGHLIGHTS

- Organic contributions from trees, herbs and C_3/C_4 graminoids are apportioned.
- δ^2H provides strong discrimination between plant functional types.
- $\delta^{13}C$ provides strong contrasts between C_3 and C_4 plants.
- δ^2H and $\delta^{13}C$ values could not differentiate aquatic and terrestrial species.
- *n*-Alkane ratios compliment isotopic discrimination.

GRAPHICAL ABSTRACT

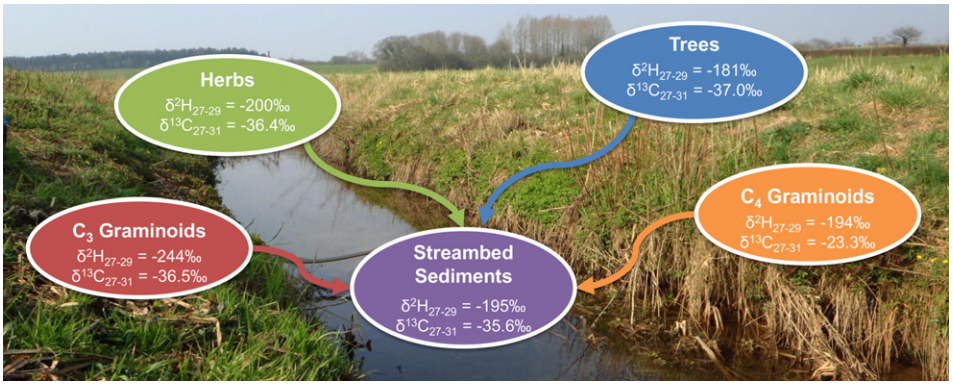

ARTICLE INFO

Article history:
Received 17 December 2014
Received in revised form 14 March 2015
Accepted 15 March 2015
Available online 24 March 2015

Editor: Eddy Y. Zeng

Keywords:
Fingerprinting
n-Alkanes
Hydrogen
Carbon
Bayesian
Mixing model

ABSTRACT

We present a novel application for quantitatively apportioning sources of organic matter in streambed sediments via a coupled molecular and compound-specific isotope analysis (CSIA) of long-chain leaf wax *n*-alkane biomarkers using a Bayesian mixing model. Leaf wax extracts of 13 plant species were collected from across two environments (aquatic and terrestrial) and four plant functional types (trees, herbaceous perennials, and C_3 and C_4 graminoids) from the agricultural River Wensum catchment, UK. Seven isotopic ($\delta^{13}C_{27}$, $\delta^{13}C_{29}$, $\delta^{13}C_{31}$, $\delta^{13}C_{27-31}$, δ^2H_{27}, δ^2H_{29}, and δ^2H_{27-29}) and two *n*-alkane ratio (average chain length (ACL), carbon preference index (CPI)) fingerprints were derived, which successfully differentiated 93% of individual plant specimens by plant functional type. The δ^2H values were the strongest discriminators of plants originating from different functional groups, with trees ($\delta^2H_{27-29} = -208‰$ to $-164‰$) and C_3 graminoids ($\delta^2H_{27-29} = -259‰$ to $-221‰$) providing the largest contrasts. The $\delta^{13}C$ values provided strong discrimination between C_3 ($\delta^{13}C_{27-31} = -37.5‰$ to $-33.8‰$) and C_4 ($\delta^{13}C_{27-31} = -23.5‰$ to $-23.1‰$) plants, but neither $\delta^{13}C$ nor δ^2H values could uniquely differentiate aquatic and terrestrial species, emphasizing a stronger plant physiological/biochemical rather than environmental control over isotopic differences. ACL and CPI complemented isotopic discrimination, with significantly longer chain lengths recorded for trees and terrestrial plants compared with herbaceous perennials and aquatic species, respectively. Application of a comprehensive Bayesian mixing model for 18 streambed sediments collected between September 2013 and March 2014 revealed considerable temporal variability in the

* Corresponding author.
E-mail address: Richard.J.Cooper@uea.ac.uk (R.J. Cooper).

http://dx.doi.org/10.1016/j.scitotenv.2015.03.058

apportionment of organic matter sources. Median organic matter contributions ranged from 22% to 52% for trees, 29% to 50% for herbaceous perennials, 17% to 34% for C_3 graminoids and 3% to 7% for C_4 graminoids. The results presented here clearly demonstrate the effectiveness of an integrated molecular and stable isotope analysis for quantitatively apportioning, with uncertainty, plant-specific organic matter contributions to streambed sediments via a Bayesian mixing model approach.

1. Introduction

Sediment fingerprinting has become a popular technique for apportioning the sources of deposited and suspended sediments across a range of aquatic environments via a mixing model approach (Mukundan et al., 2012; Guzmán et al., 2013; Walling, 2013). As the number and type of source apportionment studies have increased over recent years, there has been a shift in research focus towards re-evaluating and advancing existing fingerprinting procedures (e.g. Koiter et al., 2013; Cooper et al., 2014a; Smith and Blake, 2014; Laceby and Olley, 2014; Pulley et al., 2015). Because the majority of existing fingerprinting studies have focused solely on inorganic sediment provenance (e.g. Collins et al., 2013; Thompson et al., 2013; Wilkinson et al., 2013), the apportionment of organic matter in fluvial sediments in agricultural settings remains largely undeveloped. Understanding the origins of fluvial organic matter is important because organic material can constitute a significant percentage of the total sediment volume (e.g. Cooper et al., 2015). Furthermore, elevated organic matter concentrations are associated with enhanced transport of nutrients and heightened biological oxygen demand, thus leading to a degradation of water quality (Hilton et al., 2006; Withers and Jarvie, 2008). Whilst an understanding of the amount of organic material transported in fluvial systems can be achieved by monitoring the fluxes of dissolved (DOC) and particulate organic carbon (POC) at the catchment outlet (Alvarez-Cobelas et al., 2012; Némery et al., 2013), such measurements are unable to yield quantitative information on the specific sources of this organic load.

Addressing this matter, compound-specific isotope analysis (CSIA) has the potential to facilitate the identification of organic matter contributions to riverine sediments by exploiting differences in the stable isotopic composition amongst different plants at either the species or plant functional type level (Marshall et al., 2007). Of particular interest in this study are the carbon ($\delta^{13}C$) and hydrogen ($\delta^{2}H$) stable isotopic compositions of plant *n*-alkanes. Although *n*-alkanes represent only a small fraction of total organic matter, these compounds have unique biological origins which allow them to be used as plant-specific biomarkers of organic matter contributions (Meyers, 1997). Compared with other plant biochemical components, such as carbohydrates, amino acids and lignin, long-chain *n*-alkanes also persist in the environment due to a high resistance to degradation (Bourbonniere and Meyers, 1996), thus making them suitable conservative fingerprints for sediment source apportionment. Variability in the carbon and hydrogen isotopic compositions of plant *n*-alkanes is driven by a complex combination of differences in plant physiology/biochemistry and a range of environmental factors, including temperature, humidity, light availability, salinity and the isotopic composition of water and CO_2 (O'Leary, 1988; Farquhar et al., 1989; Sessions et al., 1999; Hou et al., 2007; Sachse et al., 2012). Importantly, this means that the degree of isotopic fractionation is theoretically unique for each individual plant, thereby allowing distinct *n*-alkane isotopic signatures to develop that can be used to differentiate between different plant types.

A number of studies have previously been successful in using the $\delta^{13}C$ isotopic signatures of soils and sediments to identify fluvial sediment contributions derived from allochthonous and autochthonous sources (e.g. McConnachie and Petticrew, 2006; Schindler Wildhaber et al., 2012; Fu et al., 2014; Wang et al., 2015), or from different land-use types based on the dominant vegetation cover (e.g. Fox and Papanicolaou, 2007; Gibbs, 2008; Blake et al., 2012; Hancock and Revill, 2013; Laceby et al., 2014). Similarly, previous studies have used molecular ratios such as the average chain length (ACL) and carbon preference index (CPI) to differentiate organic material of higher plant origin from algal or microbial contributions, or to identify petrogenic hydrocarbon inputs (e.g. Pancost and Boot, 2004; Jeng, 2006). However, to our knowledge, the usefulness of integrating both molecular ratios and compound-specific $\delta^{2}H$ and $\delta^{13}C$ values of individual organic compounds for quantifying organic matter source apportionment in stream sediments via a Bayesian mixing model approach has never been assessed. Therefore, the main objectives of this study were as follows:

(i) to assess the effectiveness of $\delta^{2}H$ and $\delta^{13}C$ values of long-chain *n*-alkanes (C_{27}, C_{29}, and C_{31}) in differentiating (a) plants derived from different functional types and (b) plants growing in aquatic and terrestrial environments;
(ii) to determine whether *n*-alkane ratios (ACL and CPI) can enhance discrimination between plant groups when used in combination with isotopic values;
(iii) to use these isotopic values and molecular ratios as fingerprints within a Bayesian mixing model to quantitatively apportion, with uncertainty, plant-specific organic matter contributions to streambed sediments.

We applied this novel CSIA fingerprinting technique to streambed sediments collected over a 7-month period between September 2013 and March 2014 from an agricultural headwater catchment of the River Wensum, Norfolk, UK.

2. Methods

2.1. Study location

The River Wensum is a nutrient enriched, lowland calcareous river system, which drains an area of 593 km^2 in Norfolk, UK. The Wensum catchment is divided into 20 sub-catchments, one of which, the 20 km^2 Blackwater sub-catchment, represents the area intensively monitored as part of the River Wensum Demonstration Test Catchment (DTC) project (Outram et al., 2014). For observational purposes, the Blackwater sub-catchment is divided into six 'mini-catchments' A to F, each of which has a bankside monitoring kiosk at the outlet. The 5.4 km^2 mini-catchment A provided the focus for this research (Fig. 1). Situated ~40 m above sea level with gentle slopes that rarely exceed 0.5°, intensively farmed arable land constitutes 92% of this headwater catchment. A 7-course crop rotation is practiced with autumn and spring sown wheat and barley, sugar beet, oilseed rape and spring beans. A small and variable amount of land is also lain down to maize for game bird cover. The remainder of mini-catchment A is covered by 3% improved grassland, 2% semi-natural grassland, 1.5% deciduous woodland, 0.5% coniferous woodland and 1% rural settlements. From May to September, emergent macrophytes dominate stream primary productivity, with this vegetation being cleared at the end of the growing season (mid-October) to improve catchment drainage and prevent winter flooding of the surrounding arable land. A weather station at the outlet to mini-catchment A recorded average precipitation totals of 808 mm $year^{-1}$ and a mean average annual temperature of 9.2 °C during April 2012–March 2014.

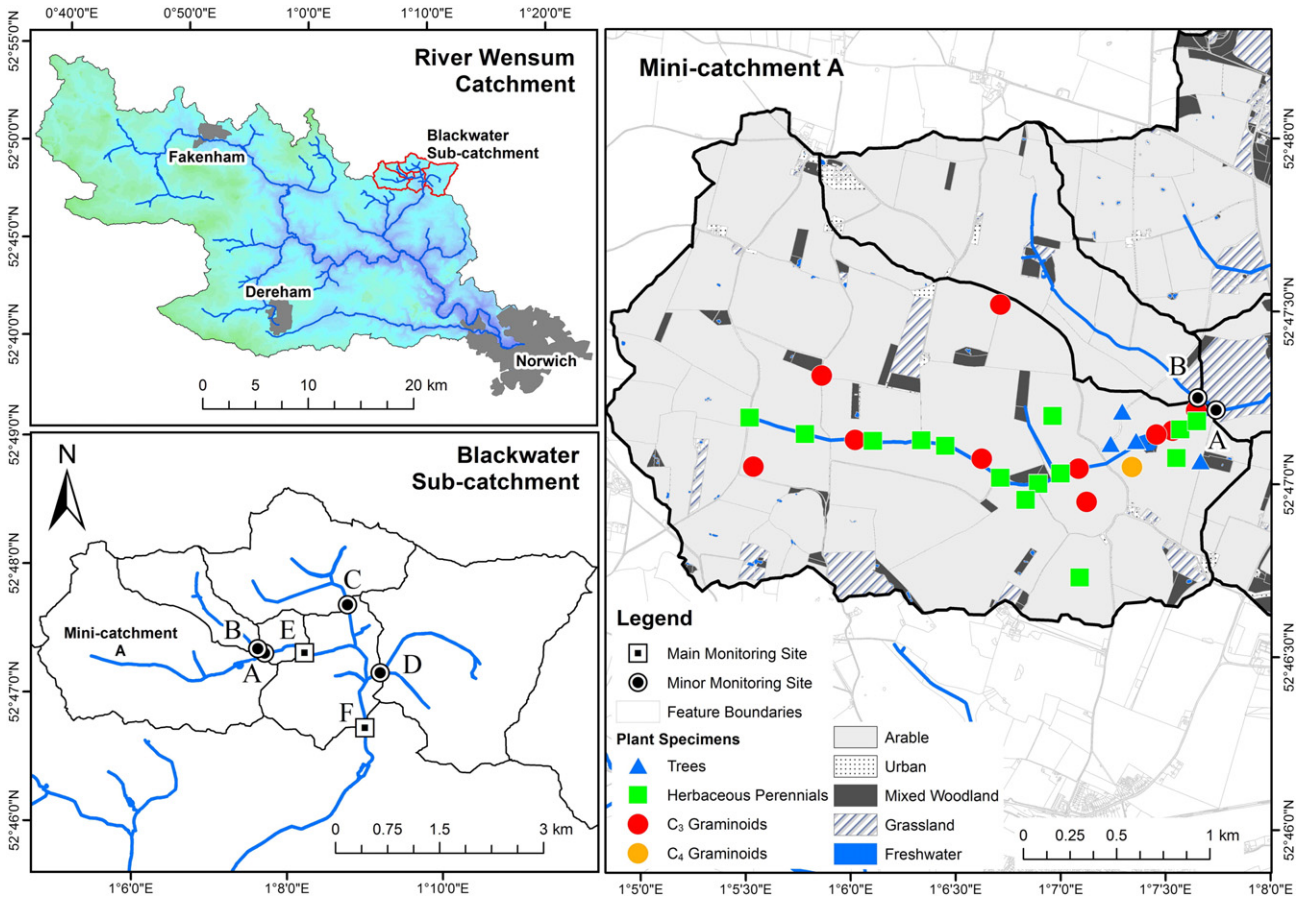

Fig. 1. The Blackwater sub-catchment of the River Wensum, Norfolk, UK, showing mini-catchments A–F, surface land cover and the locations of the collection of trees, graminoids and herbaceous perennial plants within mini-catchment A.

2.2. Sample collection and preparation

2.2.1. Streambed sediments

Streambed sediments were collected at the outlet to mini-catchment A at approximately weekly intervals between September 2013 and March 2014, yielding a total of 18 samples for analysis. This autumn to spring period was chosen as it represents the most dynamic time with respect to catchment sediment mobilization (e.g. Oeurng et al., 2011). Sediment volumes of 1 l were obtained from the streambed surface (approximately <50 mm depth) using a non-magnetic trowel that had been thoroughly washed in the stream prior to sampling. Sediments were transported back to the laboratory in sealed HDPE bottles, where upon they were immediately oven dried at 40 °C for 48–72 h. Dried sediments were lightly disaggregated using a pestle and mortar and sieved down to <63 μm to isolate the biochemically important clay–silt fraction (Horowitz, 2008) in keeping with common sediment fingerprinting practice (e.g. Walling, 2005). These fine sediments were stored in the dark at room temperature in sealed polyethylene bags prior to analysis.

2.2.2. Plant specimens

Plant leaf samples were collected across mini-catchment A during August and September 2013 for the classification of organic matter source areas. A total of 30 individual plant specimens were collected from two environments (aquatic and terrestrial) and four plant functional types (trees, herbaceous perennials, and C_3 and C_4 graminoids), and included a mixture of both cultivated and natural vegetation. For aquatic plants, 12 specimens were collected, all of which were emergent macrophytes owing to their dominance of stream biomass. These included the herbaceous perennials *Chamerion angustifolium* (rosebay willowherb), *Aegopodium podagraria* (ground elder), *Typha latifolia* (reed mace) and *Iris pseudacorus* (yellow flag iris), as well as three C_3 Poaceae graminoid specimens. For the terrestrial environment, 18 specimens were obtained, including the tree species *Crataegus monogyna* (hawthorn), *Carpinus betulus* (hornbeam), *Fraxinus excelsior* (ash) and *Acer campestre* (field maple); the herbaceous perennials *T. latifolia* (reed mace), *Raphanus sativus* (oilseed radish) and *Phaseolus vulgaris* (spring beans); the C_4 graminoid *Zea mays* (maize); the C_3 graminoid *Triticum* sp. (wheat); and a further six natural C_3 Poaceae graminoids. For each plant specimen, ~10 g of leaves were collected to provide sufficient material for replicate sample analysis. On return to the laboratory, samples were immediately frozen at −80 °C prior to being freeze-dried for 48 h and stored in the dark at room temperature in sealed polyethylene bags.

2.3. Particulate organic carbon

Particulate organic carbon (POC) concentrations for the 18 streambed sediments were determined following the procedure of Cooper et al. (2014b). 25 mg of each sediment sample was mixed into suspension with 1 l of Milli-Q water (Merck Millipore, Billerica, MA, USA) and vacuum filtered onto quartz fiber filter (QFF) papers with a particle retention rating of 99.3% at 0.45 μm. Sediment covered filters were oven dried at 105 °C for 2 h and finely ground into powders. The resulting powders were then analyzed directly by diffuse reflectance infrared Fourier transform spectroscopy (DRIFTS) to yield POC (%) concentrations. The spectrometer had previously been calibrated by partial least squares regression (PLS) against standards with known POC concentrations determined by loss-on-ignition, with POC taken to be 58% of total organic matter (Broadbent, 1953).

2.4. n-Alkane extraction

Two different techniques were required to extract aliphatic *n*-alkanes from streambed sediments and plant materials. For sediments requiring a more polar solvent to extract both the free and mineral-associated organic material, samples were mixed with Ottawa sand (SiO_2; 20–30 mesh) in a 4:1 sand–sediment ratio to improve volatilization of material prior to being run through a Dionex Accelerated Solvent Extractor (ASE) 200™ with HPLC grade dichloromethane solvent operated at 100 °C and 1500 psi. For plant specimens, alkanes were extracted by repeated sonication (3 × 10 min) of 2 g of leaf material in HPLC grade hexane. This procedure was duplicated for all 30 specimens using different leaves from the same plant to enable evaluation of isotopic variability within individual plants. Extracts from both plants and sediments were concentrated down to 1 ml under nitrogen gas in a Caliper Life Sciences TurboVap Workstation™. Final concentration down to dryness was made under nitrogen gas and the residues were re-dissolved in 1 ml hexane. The *n*-alkane extracts were purified by elution with hexane during column chromatography through a silica gel (70–230 mesh) stationary phase, and the resulting eluate was concentrated down to 1 ml under nitrogen gas in preparation for molecular and stable isotope analyses.

2.5. n-Alkane ratios

The distribution and abundance of *n*-alkanes C_{13}–C_{34} were analyzed using an Agilent Technologies 7820A gas chromatograph fitted with a flame ionization detector (GC–FID). The GC oven temperature was initially set to 50 °C for sample injection and was then ramped up at 20 °C min^{-1} between 50 °C and 150 °C, and 8 °C min^{-1} between 150 °C to 320 °C. The final temperature was held for 5 min. Individual *n*-alkanes were identified by comparison of elution times against a known *n*-C_{16} to *n*-C_{30} standard (A. Schimmelmann, Indiana University, USA). Molecular distributions were summarized by the CPI and ACL metrics following Zhang et al. (2006).

2.6. n-Alkane carbon and hydrogen isotope analyses

Compound-specific δ^2H and $\delta^{13}C$ values were determined using a Thermo Scientific™ Delta V™ Advantage isotope ratio mass spectrometer (IRMS) coupled with a GC-Isolink gas chromatograph. The GC oven temperature ramp was the same as that used for the GC–FID and reactor temperatures were set to 1000 °C for carbon and 1400 °C for hydrogen modes, respectively. All samples were run in duplicate and an *n*-alkane (C_{16} to *n*-C_{30}) standard was analyzed at the beginning and end of every 16 run sequence. $^{13}C/^{12}C$ isotopic composition was expressed relative to the Vienna Pee-Dee Belemnite (VPDB) standard and $^2H/^1H$ isotopic composition relative to Vienna Standard Mean Ocean Water (VSMOW). Only compounds ubiquitous to all sediment samples and plant specimens were used as fingerprints for source apportionment. For $\delta^{13}C$, this meant the high-molecular weight *n*-alkanes C_{27}, C_{29}, and C_{31}, whilst C_{27} and C_{29} were selected for δ^2H. Poor reproducibility of C_{31} for δ^2H meant it was excluded from the analysis. Abundance weighted C_{27}–C_{31} values for $\delta^{13}C$ and C_{27}–C_{29} values for δ^2H were included as fingerprints to account for within plant variation in chain length abundance, and were calculated as follows:

$$C_{27-29(31)}(‰) = \frac{\sum_{m=1}^{M}(\delta_m \times \alpha_m)}{\sum_{m=1}^{M}\alpha_m}$$

where δ is the isotopic value in ‰; α is the abundance in pico-volts (pV); M is the number of *n*-alkanes (three for $\delta^{13}C$, two for δ^2H); and m is the alkane index. Mean absolute errors between replicate samples (precision) were 2‰ for δ^2H_{27}, 1‰ for δ^2H_{29} and 0.1‰ for $\delta^{13}C_{27}$, $\delta^{13}C_{29}$ and $\delta^{13}C_{31}$.

2.7. Statistical source discrimination and Bayesian apportionment

The Kruskal–Wallis one-way analysis of variance and stepwise linear discriminant analysis based on the minimization of the Wilks's lambda criterion were employed to quantitatively determine the proportion of source area samples that could be correctly classified by selected isotopic values and *n*-alkane ratio fingerprints (Collins et al., 2012). Principal component (PC) analysis plots were also generated to visualize the mixing space geometry. Due to differences in plant physiology/biochemistry, the abundance of *n*-alkanes produced per unit of organic matter has been shown to vary between both species and different chain lengths within the same plant (Diefendorf et al., 2011; Bush and McInerney, 2013). Consequently, isotopic values and molecular ratios were weighted by relative *n*-alkane abundances (pV) when grouping fingerprints by source prior to running the source apportionment mixing model. This was done by passing the abundance weighted mean and covariance matrix for each source onto the Bayesian mixing model to quantitatively apportion *n*-alkane sources.

A Bayesian mixing model approach was adopted here because, unlike traditional frequentist mixing models such as IsoError (Phillips and Gregg, 2001) or IsoSource (Phillips and Gregg, 2003), Bayesian models allow for the full characterization of spatial geochemical variability, instrument precision and residual error, to yield a realistic and consistent assessment of the uncertainties associated with source apportionment estimates. This full and coherent translation of all known and residual uncertainties into parameter probability distributions represents a significant advancement over frequentist mixing models. It also averts the issue of each feasible solution being no more probable than the next — a significant limitation of the commonly used IsoSource model. This approach has already been applied to inorganic geochemical data from the same catchment (Cooper et al., 2015). Full structural details of the Bayesian model employed here are presented in the supplementary material and in Cooper et al. (2014a). In summary, samples were drawn from the joint posterior probability density function of the variables of interest:

$$p\left(S, \Phi, \Sigma^{resZ}, \mu^{\Phi}, \sigma^{2\Phi}|Y\right) \propto p\left(Y|S, \Phi, \Sigma^{resZ}\right) \cdot p(S) \cdot p\left(\Phi|\mu^{\Phi}, \sigma^{2\Phi}\right) \cdot p\left(\Sigma^{resZ}\right) \cdot p\left(\mu^{\Phi}\right) \cdot p\left(\sigma^{2\Phi}\right)$$

where Y, the concentration of each fingerprint in streambed sediment organic matter, is a function of the concentration of that fingerprint in each plant source group, S, multiplied by the proportional organic matter contribution from each source, $P = \mathrm{ILR}^{-1}(\Phi)$. Φ are isometric log-ratio (ILR) transformed proportions (P); Σ^{resZ} is the combined instrument and residual error, where instrument precision is derived empirically from repeat sample analysis; are covariance matrices; σ^2 are variances; and μ are means.

The model was run in the open source software JAGS 3.3.0 (Just Another Gibbs Sampler; Plummer, 2003) within the R environment (R Development Core Team, 2014). The model employed a Markov Chain Monte Carlo (MCMC) sampling procedure of the full parameter distributions using three parallel chains of 250,000 iterations with a 100,000 sample burn-in and a 225 sample jump length to ensure model convergence and minimize autocorrelation between sample runs. A final correction was required to convert the mixing model *n*-alkane source apportionment results into contributions of organic matter and was applied as follows:

$$P_{OM} = \frac{\frac{P_k}{\alpha_k}}{\sum_{k=1}^{K}\left(\frac{P_k}{\alpha_k}\right)}$$

where P_{OM} is the corrected contribution of organic matter from each source; P is the mixing model estimated proportion of *n*-alkanes; α is

the mean relative *n*-alkane abundance for each source; *K* is the number of sources; and *k* is the source index.

3. Results and discussion

3.1. Isotopes for discriminating plant functional types

3.1.1. Hydrogen

CSIA of the 13 plant species collected from across mini-catchment A revealed that δ^2H provided strong discrimination between some plant functional groups (Fig. 2; Table 1). Tree species (*F. excelsior*, *C. betulus*, *C. monogyna* and *A. campestre*) exhibited the most ^2H-enriched composition, with δ^2H_{27-29} values ranging from −208‰ to −164‰, with an *n*-alkane abundance weighted mean of −185‰. This contrasted strongly with the C_3 graminoids which had the lowest δ^2H_{27-29} values, ranging from −259‰ to −221‰ with an abundance weighted mean of −246‰. This is consistent with previous studies which have similarly recorded C_3 graminoids being isotopically depleted in ^2H relative to other plant types growing within the same environment (e.g. Hou et al., 2007; Eley et al., 2014). This has been linked to differences in leaf physiology between monocotyledonous graminoids and dicotyledonous trees and herbaceous plants (Helliker and Ehleringer, 2002).

The majority of species representing the herbaceous perennial group (δ^2H_{27-29} = −223‰ to −172‰), which included both natural (*T. latifolia*, *A. podagraria*, *C. angustifolium* and *I. pseudacorus*) and cultivated (*P. vulgaris* and *R. sativus*) species, overlapped with trees, though some had δ^2H_{27-29} values closer to C_3 graminoids. Despite this, the herbaceous perennials, which had an abundance weighted mean of −216‰, were significantly (*t*-test $p = 0.002$) different from both the tree and C_3 graminoid groups.

The C_4 graminoid *Z. mays* (−195‰), the only C_4 species in this study, was ^2H-enriched by ~50‰ relative to the C_3 graminoids, but overlapped with trees and herbaceous perennials. Previous studies have linked this ^2H-enrichment to shorter interveinal distances allowing for greater back diffusion of isotopically enriched water from the stomata into the veins in C_4 plants (Smith and Freeman, 2006). Overall, there existed a sizeable 94‰ range in δ^2H_{27-29} values across all 13 plant species with a clear distinction between C_3 graminoids and the other plant functional groups, thus confirming the suitability of δ^2H as an effective discriminator and fingerprint of different plant types.

3.1.2. Carbon

The dominant interspecies distinction in $\delta^{13}C_{27-31}$ values was the ~12‰ difference between the C_4 graminoid *Z. mays* and the other C_3 species (Fig. 2). This is consistent with previous studies, which have recorded similar ^{13}C-enrichment of C_4 plants compared with C_3 species and attributed this to differences in plant physiology (e.g. Pancost and Boot, 2004). The range of $\delta^{13}C_{27-31}$ values for trees (−39.2‰ to −34.2‰), C_3 graminoids (−37.5‰ to −33.8‰) and herbaceous perennials (−39.0‰ to −34.1‰) are comparable with the isotopic values recorded for long-chain *n*-alkanes from a variety of C_3 higher terrestrial plants in other studies (e.g. Collister et al., 1994; Lockheart et al., 1997; Chikaraishi and Naraoka, 2007). However, the substantial overlaps between functional groups means that there are no significant differences between trees, herbaceous perennials and C_3 grasses, thus preventing discrimination based solely upon the $\delta^{13}C$ values. This contrasts with past research that has identified differences in the $\delta^{13}C$ values between angiosperm and conifer species, for example Pedentchouk et al. (2008). However, there remains a relatively large intra-group variability that would allow individual species identification based on $\delta^{13}C_{27-31}$

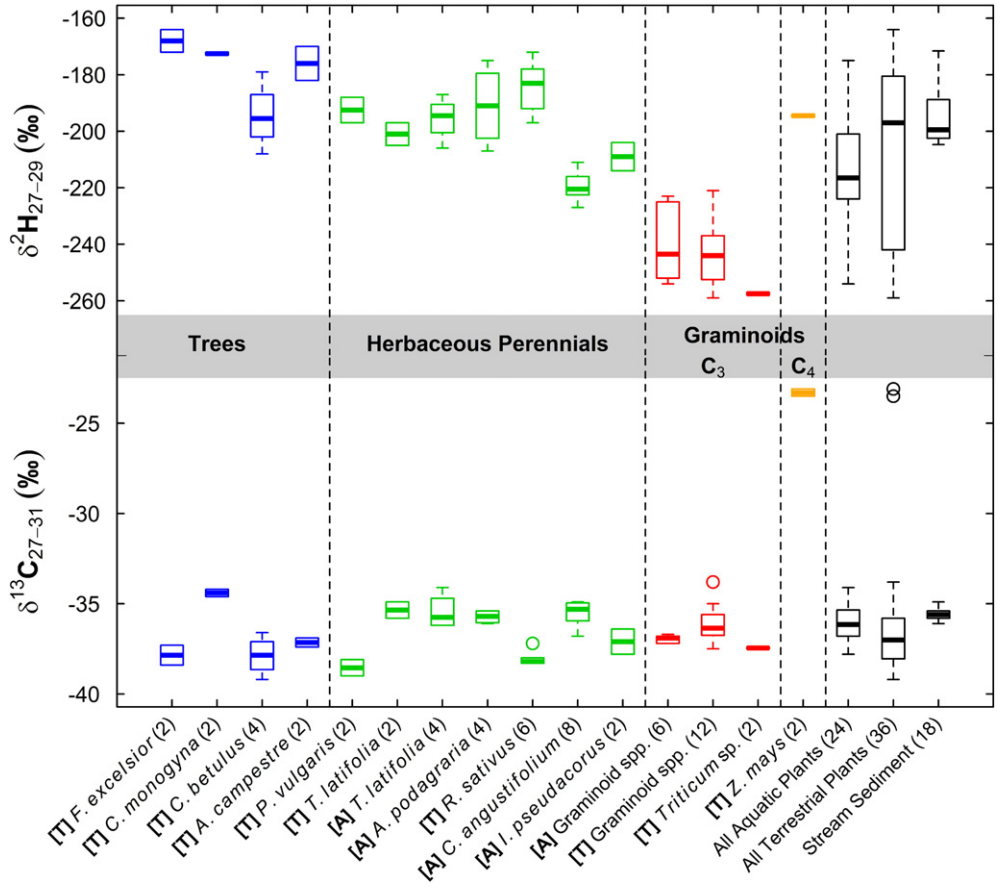

Fig. 2. Distribution of δ^2H_{27-29} and $\delta^{13}C_{27-31}$ values (‰) for streambed sediments and individual plant species arranged by plant functional type. [A] and [T] refer to aquatic and terrestrial environments, respectively. Parentheses refer to the number of specimens for each species/sediment.

Table 1
Summary of *n*-alkane ratios and isotopic compositions for streambed sediments and plant species grouped by functional type and environment. ACL is the average chain length; CPI the carbon preference index; C_{max} the most abundant *n*-alkane; μ is the mean; σ is the standard deviation. Full results for individual plant specimens are presented in supplementary Table S1.

Source/Target	Stat.	ACL	CPI	C_{max}	$\delta^{13}C_{27}$ (‰)	$\delta^{13}C_{29}$ (‰)	$\delta^{13}C_{31}$ (‰)	$\delta^{13}C_{27-31}$ (‰)	$\delta^{2}H_{27}$ (‰)	$\delta^{2}H_{29}$ (‰)	$\delta^{2}H_{27-29}$ (‰)
Streambed sediments ($n = 18$)	μ	28.9	6.5	29	−34.7	−35.7	−36.0	−35.6	−178	−203	−195
	σ	0.1	1.1	0	0.5	0.3	0.3	0.3	9	10	9
Trees ($n = 10$)	μ	29.7	13.2	31	−35.5	−37.6	−37.2	−37.0	−158	−190	−181
	σ	0.5	6.2	1	1.2	1.2	1.7	1.6	13	14	14
Herbaceous perennials ($n = 28$)	μ	28.7	12.2	29	−35.7	−36.7	−36.3	−36.4	−181	−209	−200
	σ	0.8	5.1	1	1.7	1.3	1.5	1.4	17	15	16
C_3 graminoids ($n = 20$)	μ	29.0	20.8	29	−36.1	−36.5	−36.9	−36.5	−221	−251	−244
	σ	1.1	9.9	1	1.4	1.0	0.9	0.9	16	12	12
C_4 graminoids ($n = 2$)	μ	30.4	13.4	31	−23.6	−23.7	−22.9	−23.3	−164	−200	−194
	σ	0.1	0.3	0	0.3	0.3	0.1	0.2	1	1	1
Aquatic plants ($n = 24$)	μ	28.4	12.2	29	−35.4	−36.4	−36.1	−36.0	−200	−224	−215
	σ	0.8	4.8	1	1.0	1.1	1.2	0.9	23	20	21
Terrestrial plants ($n = 36$)	μ	29.4	17.3	29	−35.4	−36.3	−36.2	−36.2	−184	−219	−209
	σ	0.8	9.2	1	3.5	3.4	3.6	3.5	30	31	31

values. For example, for herbaceous perennials where *P. vulgaris* (−38.6‰) is ^{13}C-depleted relative to the other herbaceous species (−38.3‰ to −34.1‰). The $\delta^{13}C_{27-31}$ values of the streambed sediments (−36.1‰ to −34.9‰) places them firmly within the isotopic range of the C_3 plant community, indicating limited input from C_4 plants. Because such C_3 versus C_4 discrimination cannot be obtained solely from δ^2H values, the results presented here clearly support a combined $\delta^2H/\delta^{13}C$ isotopic approach for apportioning sources of organic matter, particularly in catchments with a greater abundance of C_4 vegetation.

3.2. Isotopes for discriminating aquatic and terrestrial plants

The environment in which plants were growing exerted no obvious control over δ^2H or $\delta^{13}C$ values, as revealed by substantial overlap between the aquatic and terrestrial groups (Fig. 2). δ^2H_{27-29} values were marginally more enriched in terrestrial plants (mean (μ) = −209‰; standard deviation (σ) = 31‰) compared with aquatic growing species (μ = −215‰; σ = 21‰), however this difference was not significant (*t*-test $p = 0.3$). It is therefore not possible to differentiate terrestrial and aquatic plant groups based solely upon these isotopic values. The hydrogen isotopic composition of the streambed sediments placed them towards the terrestrial plant source group, although little can be inferred from this due to the poor source environment discrimination.

The absence of aquatic versus terrestrial discrimination implies that isotopic variability amongst the studied plants was principally driven by plant physiological and/or biochemical differences rather than the growing environment. Theoretically, one might have expected lower δ^2H values in aquatic plants compared to terrestrial species, because higher levels of humidity and water availability in aquatic environments reduce stomatal conductance and thus lower discrimination against ^2H during transpiration (Doucett et al., 2007; Sachse et al., 2012). Additionally, one might reasonably expect the δ^2H values of the stream water absorbed by aquatic plants to differ from the isotopic composition of the soil water used by terrestrial species, with the former being supplied by groundwater and the latter by more recent precipitation. However, no evidence was observed for these mechanisms with the species collected here. This can probably be explained by the shallow nature of this headwater stream (mean stage = 0.25 m), where emergent macrophytes growing >1.5 m tall dominate aquatic primary productivity. In contrast to submerged macrophytes, emergent species will be exposed to similar environmental stressors as their terrestrial equivalents, thus weakening any environment driven differences. As a consequence, we cannot rule out δ^2H and $\delta^{13}C$ as potential discriminators between aquatic and terrestrial organic matter sources, but merely highlight that differences in growing environment, particularly in headwater streams, may not impart as large an isotopic fractionation signal as physiological differences linked to plant functional type. Because of these findings, plant functional type rather than environment was pursued as the main source group classification for Bayesian source apportionment

3.3. Molecular ratios for discriminating plant types and environment

Fig. 3 presents the *n*-alkane mixing space plots of ACL and CPI for plant species grouped by (a) plant functional type and (b) environment. Despite considerable scatter between individuals of the same group, tree species had significantly (*t*-test $p < 0.001$) longer ACLs ($\mu = 29.7$; $\sigma = 0.5$; Table 1) than the herbaceous perennials ($\mu = 28.7$; $\sigma = 0.8$), whilst terrestrial plants ($\mu = 29.5$; $\sigma = 0.8$) had significantly (*t*-test $p < 0.001$) longer ACLs than the aquatic growing plants ($\mu = 28.4$; $\sigma = 0.7$). Consequently, whilst overlap between the groups prevent ACL values being used on their own to uniquely identify sources, they nevertheless assist with source identification by contributing complimentary discrimination to that provided by the isotopic data. Similarly, although there is significant overlap in the CPI values, terrestrial plants ($\mu = 17.3$; $\sigma = 9.2$) do have significantly (*t*-test $p = 0.006$) higher CPI values than aquatic plants ($\mu = 12.2$; $\sigma = 4.8$). There is also a clear distinction between terrestrial C_3 graminoids with CPI values >25 and aquatic C_3 graminoids with CPI values <15.

The ACL values for the 18 streambed sediments (range = 28.6 to 29.1) indicates that higher plants were the dominant source of *n*-alkanes in this river system. In contrast, sediment CPI values (range = 4.7 to 8.6) are towards the lower end of the range observed across all source groups. Lower CPI values can be a sign of increased algal or microbial organic contributions (Jeng, 2006; Zech et al., 2011). However, a chromatogram of mean *n*-alkane chain length distributions for all 18 streambed samples (Fig. 4) revealed sediments to be dominated by longer-chained *n*-alkanes with a strong odd-over-even predominance. Such distributions, coupled with large terrigenous-to-aquatic ratios (TAR_{HC}; range = 15.5 to 64.5), are indicative of higher terrestrial plant origins (Bourbonniere and Meyers, 1996; McDuffee et al., 2004). This allows algae and bacteria to be excluded as major organic matter sources during this autumn to spring period. Low CPI values can also indicate contributions from ancient organic matter weathered out of the soil profile (Pancost and Boot, 2004). Depending on its age, this ancient material may reflect relic plant communities that bear little resemblance to the modern intensive arable system and therefore would not have been represented by the plant specimens collected here to classify source groups. Petroleum washed off metaled roads and transported into the stream during heavy rainfall events could also explain these low CPI values.

3.4. Statistical discrimination of isotopic and molecular ratio fingerprints

Principal component analysis (Fig. 5) revealed that 95.1% of the variability between the plant species could be explained by the first three

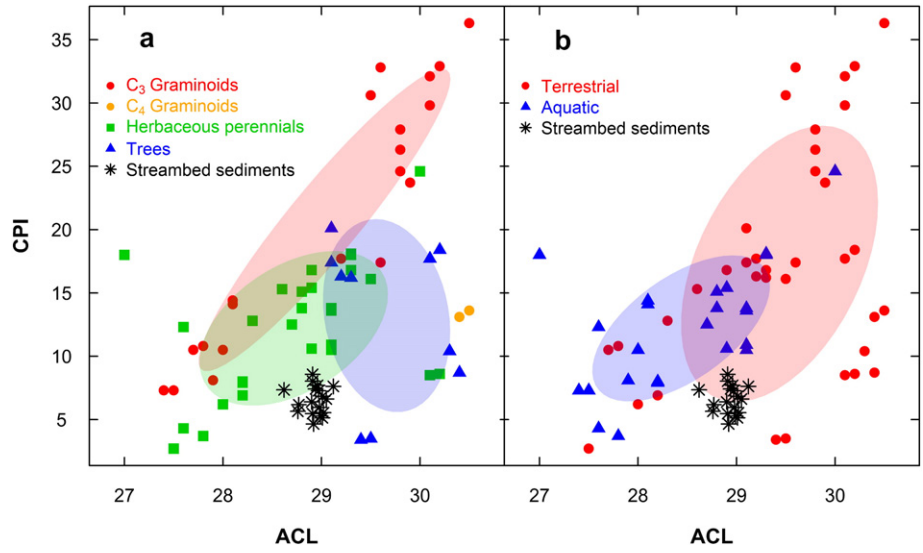

Fig. 3. Average chain length (ACL) and carbon preference index (CPI) mixing space plots for streambed sediments and individual plant specimens grouped by (a) plant functional type and (b) environment. Shaded ellipsoids encompass 50% of group range.

components when combining all nine of the measured isotopic and *n*-alkane ratio fingerprints ($\delta^{13}C_{27}$, $\delta^{13}C_{29}$, $\delta^{13}C_{31}$, $\delta^{13}C_{27-31}$, $\delta^{2}H_{27}$, $\delta^{2}H_{29}$, $\delta^{2}H_{27-29}$, ACL, and CPI). PC1, which explained 43.69% of data variance, weighed most heavily upon the four $\delta^{13}C$ fingerprints, with the more positive $\delta^{13}C$ values of C_4 graminoids providing the greatest distinction. The second principal component (33.92% of data variance) highlighted hydrogen isotope composition as a powerful discriminator between the ^{2}H-depleted C_3 graminoids and the comparatively ^{2}H-enriched herbaceous perennials and trees. In the third component (17.51% of variance), ACL was the dominant discriminator, with higher ACL values for trees helping to distinguish this group from the herbaceous perennials. CPI was also an important distinguishing metric, with values increasing from herbaceous perennials ($\mu = 12.2$), to trees ($\mu = 13.2$) and finally C_3 graminoids ($\mu = 20.8$).

The Kruskal–Wallis one-way analysis of variance revealed that eight out of the nine fingerprints could successfully differentiate between plant functional types at the 95% significance level (Table 2). Whilst previous studies have used failure to pass this test as a fingerprint rejection criterion in traditional frequentist source apportionment studies (e.g. Collins et al., 2012; Evrard et al., 2013), other research has demonstrated that maximizing the number of fingerprints used in Bayesian mixing models can help to significantly improve differentiation and reduce model uncertainties, provided the fingerprints contribute some discriminatory information (Parnell et al., 2010). All nine fingerprints were therefore passed onto the Bayesian mixing model. In combination, the minimization of Wilks's lambda procedure revealed 93.1% of plant specimens could be correctly classified by plant functional type from these nine fingerprints, with $\delta^{13}C_{31}$ and $\delta^{2}H_{27-29}$ being the two most important discriminants (highest *F*-values; Table 2).

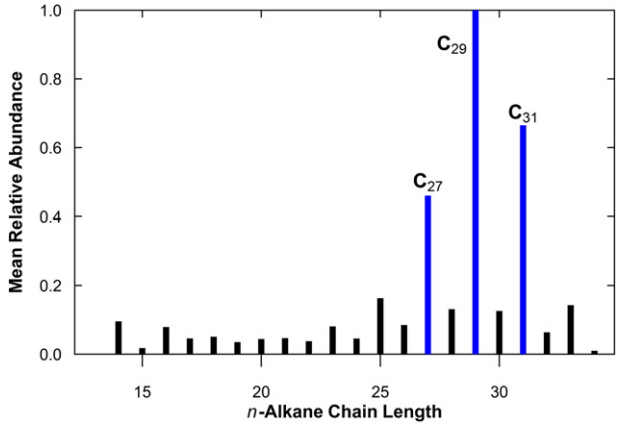

Fig. 4. Chromatogram of the mean *n*-alkane chain length distribution for the 18 streambed sediment samples collected between September 2013 and March 2014, expressed relative to C_{29}. High-molecular weight *n*-alkanes ubiquitous to all samples and selected as isotopic fingerprints are labeled.

3.5. Application of the Bayesian source apportionment mixing model

The 7-month time-series of organic matter source contributions to streambed sediments, as estimated by the nine fingerprint Bayesian mixing model, are presented in Fig. 6. Over the entire September 2013 to March 2014 period, POC concentrations varied between 3% and 7% of total sediment volume, which is considerably lower than the 10%–13% recorded for suspended particulate matter (SPM) collected at the same time from the same site (data not shown). Although *n*-alkanes represent only a small fraction of this total organic material, their conservative nature means we can work on the assumption that the sources of *n*-alkane biomarkers are representative of the sources of the entire organic matter content of the streambed sediments. In this regard, herbaceous perennials were estimated to account for a mean 39% (13–65% at the 95% credible interval) of sediment organic matter over this 7-month period, with a further 33% (12–54%) from trees, 26% (7–46%) from C_3 graminoids and just 4% (0–16%) from C_4 graminoids. The high contribution from herbaceous plants is consistent with the dominance of emergent herbaceous macrophytes in the stream channel during the summer months. Similarly, whilst only 1.5% of the catchment is deciduous woodland, significant tree contribution was not surprising given the proximity of deciduous trees to the stream. There is also an extensive network of *C. monogyna* and *A. campestre* hedgerows across the catchment, which most likely contributed significant quantities of tree derived organic material following autumn and winter leaf fall.

In spite of the relatively low precision of the proportional contributions, which arises as a consequence of the comprehensive Bayesian treatment of all perceived uncertainties (Cooper et al., 2014a), considerable temporal variability in apportionment estimates was still apparent. Median contributions from trees ranged from 22% to 52% (3% to 70% at the 95% credible interval), herbaceous perennials from 29% to 50% (2% to 67%) and C_3 graminoids from 17% to 34% (4% to 58%) across the 7-month period. By contrast, median C_4 graminoid contributions were consistently low at 3% to 7% (0% to 22%). As expected from the PC analysis (Fig. 5), variability in sediment $\delta^{2}H_{27-29}$ values appeared to exert

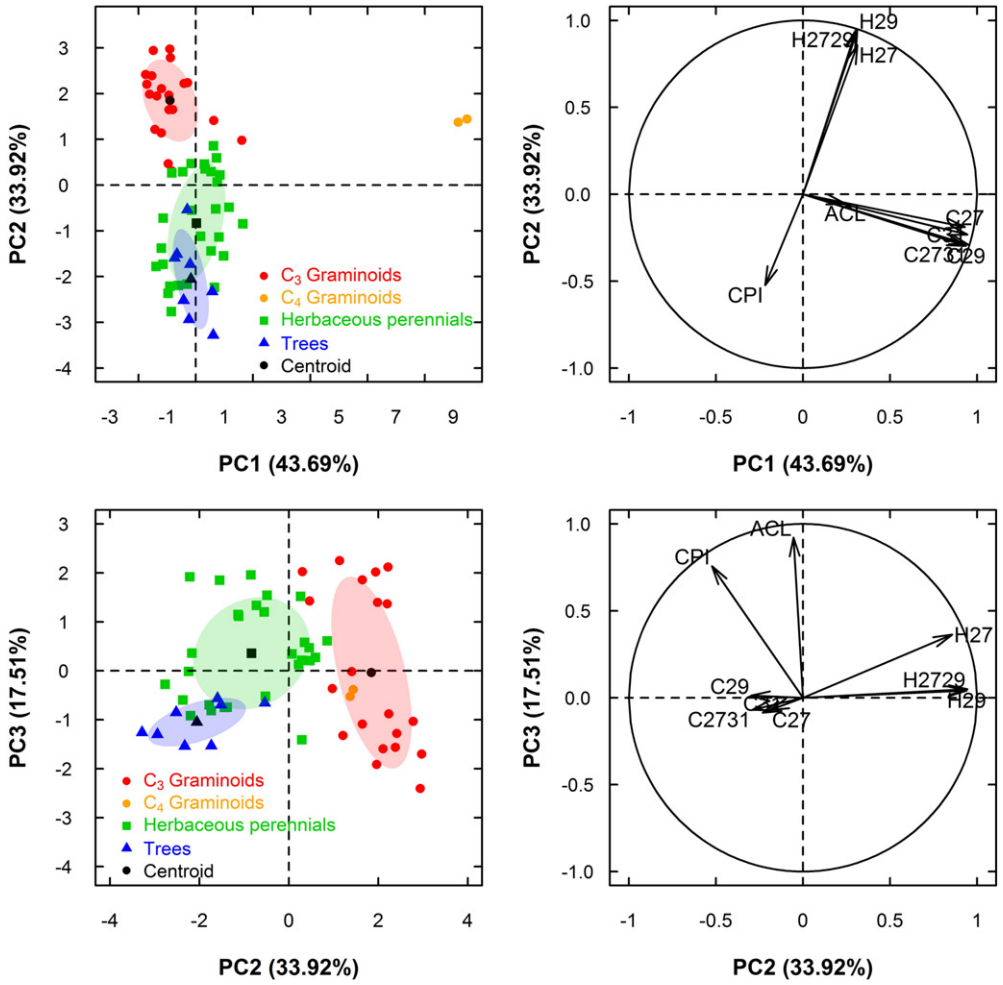

Fig. 5. Principal component analysis of plant functional type sources (left) and fingerprint loadings (right) for the first three components. Shaded ellipsoids encompass 50% of group range.

the dominant control over estimated source contributions. Increases in δ^2H_{27-29} values were generally associated with increases in tree contribution and declines in C_3 graminoid supply, reflecting the more positive δ^2H values of tree-derived organic material (Fig. 2). None of the source contributions correlated with either stage or weekly precipitation totals.

Despite this variability in source apportionment estimates at a weekly timescale (Fig. 6), there was no strong seasonality to estimated contributions, in contrast to what one might intuitively expect considering the strong seasonal nature of plant growth. Whilst tree contribution does increase by 17% during early October, which may relate to autumn leaf fall, this cannot directly explain the peak in tree contribution at 52% during mid-February 2014. Similarly, whilst herbaceous perennial contribution is marginally higher (median = 43%) during the September to November die-back of emergent macrophytes than during the December to March period (median = 38%), the trend is not significant within the 95% uncertainty intervals of the model.

Previous research has shown the δ^2H values of individual plant species can vary seasonally in response to environmental stressors (e.g. temperature) by up to 44‰ (Pedentchouk et al., 2008; Eley et al., 2014). Whilst we potentially see evidence for this seasonality here, with the most isotopically depleted sediment δ^2H_{27-29} values occurring during the colder winter months (~−200‰) and the most enriched values occurring in autumn and spring (~−185‰) (Fig. 6), this does not translate into seasonality in apportionment estimates. On reflection, the lack of seasonal apportionment sensitivity most likely reflects the composition of deposited streambed sediments being inherently less dynamic and responsive to catchment processes than fine grained SPM, for example. Streambed sediments represent a cumulative

Table 2
Kruskal–Wallis one-way analysis of variance and minimization of fingerprint discrimination statistics.

Fingerprint property	Kruskal–Wallis		Minimization of Wilks's lambda				
	H-value	*P*-value	Selection step	Wilks's Lambda	*F*-value	Cumulative *p*-value	Cumulative % of sources correctly classified
$\delta^{13}C_{31}$	10.14	0.017	1	0.167	89.9	<0.001	51.7
δ^2H_{27-29}	42.32	<0.000	2	0.043	68.0	<0.001	82.8
ACL	13.48	0.004	3	0.034	42.3	<0.001	84.5
$\delta^{13}C_{27}$	7.39	0.060	4	0.028	32.3	<0.001	89.7
δ^2H_{29}	40.08	<0.000	5	0.024	26.4	<0.001	93.1
$\delta^{13}C_{27-31}$	8.24	0.041	6	0.021	22.6	<0.001	93.1
δ^2H_{27}	41.95	<0.000	7	0.019	19.8	<0.001	93.1
$\delta^{13}C_{29}$	9.18	0.027	8	0.017	17.6	<0.001	93.1
CPI	8.34	0.039	9	0.016	15.5	<0.001	93.1

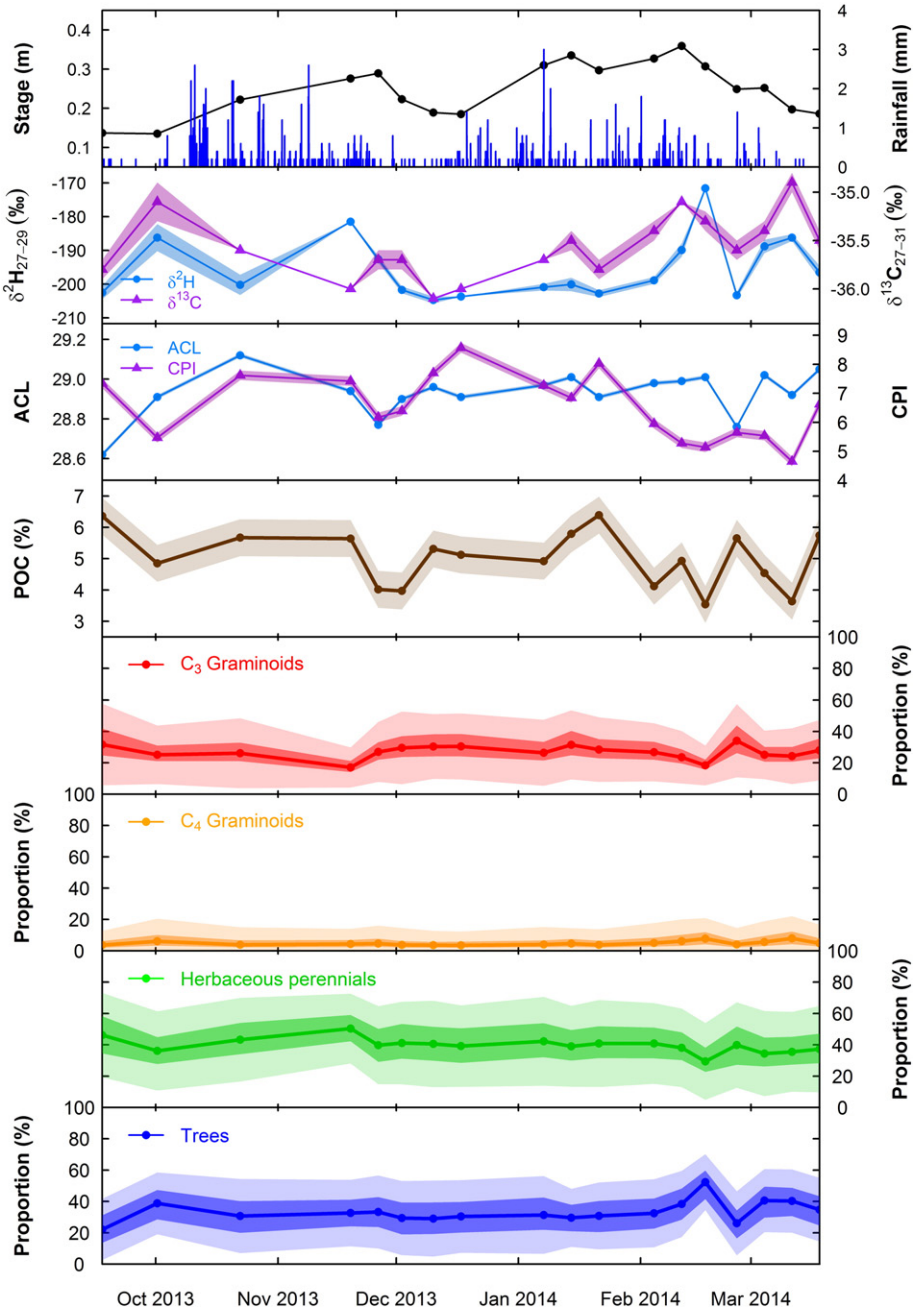

Fig. 6. Time-series of organic matter source apportionment estimates and streambed sediment fingerprints for the River Wensum during September 2013–March 2014. Dark shading and light shading around median source apportionment estimates represent the 50% and 95% Bayesian credible intervals, respectively. Shading around isotopic values and ACL, CPI and POC measurements represents instrument error.

composite of material deposited over a number of days, weeks or months. As such, the delivery of a pulse of δ^2H enriched autumn tree leaf litter to the river, which may be instantly detectable in SPM, would form just the most recent quantitatively insignificant addition to a larger pool of accumulated organic detritus deposited on the streambed. Additionally, autumn leaf litter may remain on the ground for a prolonged period of time before precipitation of sufficient intensity is capable of initiating surface runoff to entrain and transport this organic material to the stream channel.

3.6. Significance and further research

The novel data presented here clearly demonstrate that an integrated molecular and carbon and hydrogen CSIA of leaf wax *n*-alkanes is an effective approach for quantitatively apportioning plant-specific organic matter contributions to streambed sediments within a Bayesian uncertainty framework. In particular, the δ^2H values of leaf waxes proved to be an effective biomarker for differentiating between individual plant species based upon their broad functional type, whilst $\delta^{13}C$ values and *n*-alkane ratios provided complimentary discrimination based on C_3/C_4 physiological differences and different environments, respectively. In contrast to inorganic fingerprints which have commonly been used to discriminate sediment sources based on catchment geology and soil type in previous sediment source apportionment studies (e.g. Martínez-Carreras et al., 2010; D'Haen et al., 2012), these isotopic differences in *n*-alkane composition offer considerable potential to quantify land-use specific contributions to fluvial organic matter. In this respect, future research could usefully examine if soils under

particular plant types are tagged with unique δ^2H and $\delta^{13}C$ signatures, which may allow these isotopes to be used as direct land-use specific soil erosion tracers. There would also be utility in applying these techniques to SPM collected at high-temporal resolution during precipitation events as a means of better understanding organic matter provenance and transport during dynamic high-flow conditions. Finally, examination of a variety of natural and cultivated plant species would allow for an assessment of the effectiveness of both $\delta^{13}C$ and δ^2H as discriminators of crops and natural vegetation, which could assist with the apportioning of anthropogenic organic matter inputs to fluvial environments.

4. Conclusions

Organic matter is an important constituent of the particulate material transported in fluvial systems, yet techniques capable of quantitatively apportioning its origin have largely been overlooked by the sediment fingerprinting community. Addressing this deficiency, we successfully demonstrate how a novel, combined molecular and $\delta^{13}C$ and δ^2H compound-specific stable isotope analysis of *n*-alkane plant lipid extracts can be used to apportion plant-specific organic matter contributions to fine (<63 μm) streambed sediments in a lowland, arable catchment. From the lipid extracts of 18 streambed sediments and 30 individual plant specimens collected from across two environments (aquatic and terrestrial) and four plant functional types (trees, herbaceous perennials, and C_3 and C_4 graminoids), seven isotopic values ($\delta^{13}C_{27}$, $\delta^{13}C_{29}$, $\delta^{13}C_{31}$, $\delta^{13}C_{27-31}$, δ^2H_{27}, δ^2H_{29} and δ^2H_{27-29}) and two *n*-alkane ratios (ACL and CPI) were derived, which were capable of successfully differentiating 93.1% of plant specimens by functional group. δ^2H_{27-29} proved to be the dominant discriminator of plants originating from different functional types, with the largest contrasts arising between trees (−208‰ to −164‰) and C_3 graminoids (259‰ to −221‰). $\delta^{13}C_{27-31}$ provided effective discrimination between the ^{13}C-enriched C_4 graminoids and C_3 plants. Neither δ^2H nor $\delta^{13}C$ could robustly differentiate aquatic and terrestrial plants, emphasizing a stronger physiological rather than growing environment control over isotopic fractionation. The ACL and CPI were, however, more successful at differentiating terrestrial and aquatic plants, indicating that such molecular ratios can complement source area identification when used in combination with isotopic values. Bayesian mixing model source apportionment results took full account of the uncertainties present whilst revealing considerable temporal variability in plant contributions to streambed sediments during the 7-month period between September 2013 and March 2014. Median contributions ranged from 22% to 52% for trees, 29% to 50% for herbaceous perennials, 17% to 34% for C_3 graminoids and 3% to 7% from C_4 graminoids, with apportionment exhibiting no apparent seasonality. The results of this study have clearly demonstrated the effectiveness of an integrated molecular and compound-specific carbon and hydrogen isotope analysis for identifying plant-specific contributions to streambed sediment organic matter via a Bayesian mixing model approach. Future research should further investigate the potential of δ^2H and $\delta^{13}C$ as direct erosion tracers of soils under different land cover types.

Acknowledgments

RJC acknowledges financial support from a NERC BGS CASE studentship (NE/J500069/1). TK is funded, through IRI THESys, by the German Excellence Initiative. Further information on the Bayesian mixing model structure and complete isotopic data for the plants is presented in the supplementary material. The authors would like to thank Yvette Eley and Rebecca Baldwin for laboratory assistance; Jenny Stevenson, Simon Ellis and Zanist Hama-Aziz for fieldwork support; and Gilla Suennenberg for providing the GIS data. We are grateful to Salle Farms Co. for their cooperation in granting land access. We thank three anonymous reviewers for their constructive comments which helped improve an earlier version of this manuscript. This paper is published with the permission of the Executive Director of the British Geological Survey (Natural Environment Research Council).

Appendix A. Supplementary data

Supplementary data to this article can be found online at http://dx.doi.org/10.1016/j.scitotenv.2015.03.058.

References

Alvarez-Cobelas, M., Angeler, D.G., Sánchez-Carrillo, S., Almendros, G., 2012. A worldwide view of organic carbon export from catchments. Biogeochemistry 107, 275–293. http://dx.doi.org/10.1007/s10533-010-9553-z.

Blake, W.H., Ficken, K.J., Taylor, P., Russell, M.A., Walling, D.E., 2012. Tracing crop-specific sediment sources in agricultural catchments. Geomorphology 139–140, 322–329. http://dx.doi.org/10.1016/j.geomorph.2011.10.036.

Bourbonniere, R.A., Meyers, P.A., 1996. Sedimentary geolipid records of historical changes in the watersheds and productivities of lakes Ontario and Erie. Am. Soc. Limnol. Oceanogr. 41, 352–359.

Broadbent, F.E., 1953. The soil organic fraction. Adv. Agron. 5, 153–183.

Bush, R.T., McInerney, F.A., 2013. Leaf wax *n*-alkane distributions in and across modern plants: implications for paleoecology and chemotaxonomy. Geochim. Cosmochim. Acta 117, 161–179. http://dx.doi.org/10.1016/j.gca.2013.04.016.

Chikaraishi, Y., Naraoka, H., 2007. $\delta^{13}C$ and δD relationships among three *n*-alkyl compound classes (*n*-alkanoic acid, *n*-alkane and *n*-alkanol) of terrestrial higher plants. Org. Geochem. 38, 198–215. http://dx.doi.org/10.1016/j.orggeochem.2006.10.003.

Collins, A.L., Zhang, Y., Walling, D.E., Grenfell, S.E., Smith, P., Grischeff, J., Locke, A., Sweetapple, A., Brogden, D., 2012. Quantifying fine-gained sediment sources in the River Axe catchment, southwest England: application of a Monte Carlo numerical modelling framework incorporating local and genetic algorithm optimization. Hydrol. Process. 26, 1962–1983. http://dx.doi.org/10.1002/hyp.8283.

Collins, A.L., Zhang, Y.S., Duethmann, D., Walling, D.E., Black, K.S., 2013. Using a novel tracing-tracking framework to source fine-grained sediment loss to watercourses at sub-catchment scale. Hydrol. Process. 27, 959–974. http://dx.doi.org/10.1002/hyp.9652.

Collister, J.W., Rieley, G., Stern, B., Eglinton, G., Fry, B., 1994. Compound-specific $\delta^{13}C$ analyses of leaf lipids from plants with differing carbon dioxide metabolisms. Org. Geochem. 21, 619–627.

Cooper, R.J., Krueger, T., Hiscock, K.M., Rawlins, B.G., 2014a. Sensitivity of fluvial sediment source apportionment to mixing model assumptions: a Bayesian model comparison. Water Resour. Res. 50, 9031–9047. http://dx.doi.org/10.1002/2014WR016194.

Cooper, R.J., Rawlins, B.G., Lézé, B., Krueger, T., Hiscock, K., 2014b. Combining two filter paper-based analytical methods to monitor temporal variations in the geochemical properties of fluvial suspended particulate matter. Hydrol. Process. 28, 4042–4056. http://dx.doi.org/10.1002/hyp.9945.

Cooper, R.J., Krueger, T., Hiscock, K.M., Rawlins, B.G., 2015. High-temporal resolution fluvial sediment source fingerprinting with uncertainty: a Bayesian approach. Earth Surf. Process. Landf. 40, 78–92. http://dx.doi.org/10.1002/esp.3621.

D'Haen, K., Verstraeten, G., Dusar, B., Degryse, P., Haex, J., Waelkens, M., 2012. Unravelling changing sediment sources in a Mediterranean mountain catchment: a Bayesian fingerprinting approach. Hydrol. Process. 27, 896–910. http://dx.doi.org/10.1002/hyp.9399.

Diefendorf, A.F., Freeman, K.H., Wing, S.L., Graham, H.V., 2011. Production of *n*-alkyl lipids in living plants and implications for the geologic past. Geochim. Cosmochim. Acta 75, 7478–7485. http://dx.doi.org/10.1016/j.gca.2011.09.028.

Doucett, R.R., Marks, J.C., Blinn, D.W., Caron, M., Hungate, B.A., 2007. Measuring terrestrial subsidies to aquatic food webs using stable isotopes of hydrogen. Ecology 88, 1587–1592. http://dx.doi.org/10.1890/06-1184.

Eley, Y., Dawson, L., Black, S., Andrews, J., Pedentchouk, N., 2014. Understanding $^2H/^1H$ systematics of leaf wax *n*-alkanes in coastal plants at Stiffkey saltmarsh, Norfolk, UK. Geochim. Cosmochim. Acta 128, 13–28. http://dx.doi.org/10.1016/j.gca.2013.11.045.

Evrard, O., Poulenard, J., Némery, J., Ayrault, S., Gratiot, N., Duvert, C., Prat, C., Lefèvre, I., Bonté, P., Esteves, M., 2013. Tracing sediment sources in a tropical highland catchment of central Mexico by using conventional and alterative fingerprinting methods. Hydrol. Process. 27, 911–922. http://dx.doi.org/10.1002/hyp.9421.

Farquhar, G.D., Ehleringer, J.R., Hubick, K.T., 1989. Carbon isotope discrimination and photosynthesis. Annu. Rev. Plant Physiol. Plant Mol. Biol. 40, 503–537.

Fox, J.F., Papanicolaou, A.N., 2007. The use of carbon and nitrogen isotopes to study watershed erosion processes. J. Am. Water Resour. Assoc. 43, 1047–1064. http://dx.doi.org/10.1111/j.1752-1688.2007.00087.x.

Fu, Y., Tang, C., Li, J., Zhao, Y., Zhong, W., Zeng, X., 2014. Sources and transport of organic carbon from the Dongjiang River to the Humen outlet of the Pearl River, southern China. J. Geogr. Sci. 24, 143–158. http://dx.doi.org/10.1007/s1142-014-1078-2.

Gibbs, M.M., 2008. Identifying source soils in contemporary estuarine sediments: a new compound-specific isotope method. Estuar. Coasts 31, 344–359. http://dx.doi.org/10.1007/s12237-007-9012-9.

Guzmán, G., Quinton, J.N., Nearing, M.A., Mabit, L., Gómez, J.A., 2013. Sediment tracers in water erosion studies: current approaches and challenges. J. Soils Sediments 13, 816–833. http://dx.doi.org/10.1007/s11368-013-0659-5.

Hancock, G.J., Revill, A.T., 2013. Erosion source discrimination in a rural Australian catchment using compound-specific isotope analysis (CSIA). Hydrol. Process. 27, 923–932. http://dx.doi.org/10.1002/hyp.9466.
Helliker, B.R., Ehleringer, J.R., 2002. Grass blades as tree rings: environmentally induced changes in the oxygen isotope ratio of cellulose along the length of grass blades. New Phytol. 155, 417–424. http://dx.doi.org/10.1046/j.1469-8137.2002.00480.x.
Hilton, J., O'Hare, M., Bowes, M.J., Jones, J.I., 2006. How green is my river? A new paradigm of eutrophication in rivers. Sci. Total Environ. 365, 66–83. http://dx.doi.org/10.1016/j.scitotenv.2006.02.055.
Horowitz, A.J., 2008. Determining annual suspended sediment and sediment-associated trace element and nutrient fluxes. Sci. Total Environ. 400, 315–343. http://dx.doi.org/10.1016/j.scitotenv.2008.04.022.
Hou, J., D'Andrea, W.J., MacDonald, D., Huang, Y., 2007. Hydrogen isotopic variability in leaf waxes among terrestrial and aquatic plants around Blood Pond, Massachusetts (USA). Org. Geochem. 38 (977), 984. http://dx.doi.org/10.1016/j.orggeochem.2006.12.009.
Jeng, W.-L., 2006. Higher plant *n*-alkane average chain length as an indicator of petrogenic hydrocarbon contamination in marine sediments. Mar. Chem. 102, 242–251. http://dx.doi.org/10.1016/j.marchem.2006.05.001.
Koiter, A.J., Owens, P.N., Petticrew, E.L., Lobb, D.A., 2013. The behavioral characteristics of sediment properties and their implications for sediment fingerprinting as an approach for identifying sediment sources in river basins. Earth Sci. Rev. 125, 24–42. http://dx.doi.org/10.1016/j.earscirev.2013.05.009.
Laceby, J.P., Olley, J., 2014. An examination of geochemical modelling approaches to tracing sediment sources incorporating distribution mixing and elemental correlations. Hydrol. Process. http://dx.doi.org/10.1002/hyp.10287.
Laceby, J.P., Olley, J., Pietsch, T.J., Sheldon, F., Bunn, S.E., 2014. Identifying subsoil sediment sources with carbon and nitrogen stable isotope ratios. Hydrol. Process. http://dx.doi.org/10.1002/hyp.10311.
Lockheart, M.J., Van Bergen, P.F., Evershed, R.P., 1997. Variations in the stable carbon isotope compositions of individual lipids from the leaves of modern angiosperms: implications for the study of higher land plant-derived sedimentary organic matter. Org. Geochem. 26, 137–153.
Marshall, J.D., Brooks, J.R., Lajtha, K., 2007. Sources of variation in the stable isotopic composition of plants. In: Michener, R., Lajtha, K. (Eds.), Stable Isotopes in Ecology and Environmental Science. Blackwell Publishing, pp. 22–60.
Martínez-Carreras, N., Krein, A., Udelhoven, T., Gallart, F., Iffly, J.F., Hoffmann, L., Pfister, L., Walling, D.E., 2010. A rapid spectral-reflectance-based fingerprinting approach for documenting suspended sediment sources during storm runoff events. J. Soils Sediments 10, 400–413. http://dx.doi.org/10.1007/s11368-009-0162-1.
McConnachie, J.L., Petticrew, E.L., 2006. Tracing organic matter sources in riverine suspended sediments: implications for fine sediment transfers. Geomorphology 79, 13–26. http://dx.doi.org/10.1016/j.geomorph.2005.09.011.
McDuffee, K.E., Eglinton, T.I., Sessions, A.L., Sylva, S., Wagner, T., Hayes, J.M., 2004. Rapid analysis of ^{13}C in plant-wax *n*-alkanes for reconstruction of terrestrial vegetation signals from aquatic sediments. Geochem. Geophys. Geosyst. 5 (10), Q10004. http://dx.doi.org/10.1029/2004GC000772.
Meyers, P.A., 1997. Organic geochemical proxies of paleoceanographic, paleolimnologic, and paleoclimatic processes. Org. Geochem. 27, 213–250.
Mukundan, R., Walling, D.E., Gillis, A.C., Slattery, M.C., Radcliffe, D.E., 2012. Sediment source fingerprinting: transforming from a research tool to a management tool. J. Am. Water Resour. Assoc. 48, 1241–1257. http://dx.doi.org/10.1111/j.1752-1688.2012.00685.x.
Némery, J., Mano, V., Cornella, Etcher, H., Mostar, F., Me beck, M., Belled, P., Pore, A., 2013. Carbon and suspended sediment transport in an impounded alpine river (Isère, France). Hydrol. Process. 27, 2498–2508. http://dx.doi.org/10.1002/hyp.9387.
O'Leary, M.H., 1988. Carbon isotopes in photosynthesis. Bioscience 38, 328–336.
Oeurng, C., Savage, S., Cornel, A., Manuel, E., Etcher, H., Sánchez-Pérez, J.-M., 2011. Fluvial transport of suspended sediments and organic matter during flood events in a large agricultural catchment in southwest France. Hydrol. Process. 25, 2365–2378. http://dx.doi.org/10.1002/hyp.7999.
Outram, F.N., Lloyd, C.E.M., Jonczyk, J., Benskin, C.M.H., Grant, F., Perks, M.T., Deasy, C., Burke, S.P., Collins, A.L., Freer, J., Haygarth, P.M., Hiscock, K.M., Johnes, P.J., Lovett, A.L., 2014. High-frequency monitoring of nitrogen and phosphorus response in three rural catchments to the end of the 2011–2012 drought in England. Hydrol. Earth Syst. Sci. 18, 3429–3448. http://dx.doi.org/10.5194/hess-18-3429-2014.
Pancost, R.D., Boot, C.S., 2004. The palaeoclimatic utility of terrestrial biomarkers in marine sediments. Mar. Chem. 92, 239–261. http://dx.doi.org/10.1016/j.marchem.2004.06.029.
Parnell, A.C., Inger, R., Bearhop, S., Jackson, A.L., 2010. Source partitioning using stable isotopes: coping with too much variation. PLoS ONE 5, e9672. http://dx.doi.org/10.1371/journal.pone.0009672.
Pedentchouk, N., Sumner, W., Tipple, B., Pagani, M., 2008. $\delta^{13}C$ and $\delta^{2}H$ compositions of *n*-alkanes from modern angiosperms and conifers: an experimental set up in central Washing State, USA. Org. Geochem. 39, 1066–1071. http://dx.doi.org/10.1016/j.orggeochem.2008.02.005.
Phillips, D.L., Gregg, J.W., 2001. Uncertainty in source partitioning using stable isotopes. Oecologia 127, 171–179. http://dx.doi.org/10.1007/s004420000578.
Phillips, D.L., Gregg, J.W., 2003. Source partitioning using stable isotopes: coping with too many sources. Oecologia 136, 261–269. http://dx.doi.org/10.1007/s00442-003-1218-3.
Plummer, M., 2003. JAGS: a program for analysis of Bayesian graphical models using Gibbs sampling. Proceedings of the 3rd International Workshop on Distributed Statistical Computing, Vienna, Austria.
Pulley, S., Foster, I., Antunes, P., 2015. The uncertainties associated with sediment fingerprinting suspended and recently deposited fluvial sediment in the Nene river basin. Geomorphology 228, 303–319. http://dx.doi.org/10.1016/j.geomorph.2014.09.016.
R Development Core Team, 2014. R: A Language and Environment for Statistical Computing. R Foundation for Statistical Computing, Vienna, Austria (http://www.R-project.org).
Sachse, D., Billault, I., Bowen, G., Chikaraishi, Y., Dawson, T., Feakins, S., Freeman, K., Magill, C., McInerney, F., van der Meer, M., Polissar, P., Robins, R., Sachs, J., Schmidt, H., Sessions, A., White, J., West, J., Kahmen, A., 2012. Molecular paleohydrology: interpreting the hydrogen-isotopic composition of lipid biomarkers from photosynthesizing organisms. Annu. Rev. Earth Planet. Sci. 40, 221–249. http://dx.doi.org/10.1146/annurev-earth-042711-105535.
Schindler Wildhaber, Y., Liechti, R., Alewell, C., 2012. Organic matter dynamics and stable isotope signature as tracers of the sources of suspended sediment. Biogeosciences 9, 1985–1996. http://dx.doi.org/10.5194/bg-9-1985-2012.
Sessions, A.L., Burgoyne, T.W., Schimmelmann, A., Hayes, J.M., 1999. Fractionation of hydrogen isotopes in lipid biosynthesis. Org. Geochem. 30, 1193–1200. http://dx.doi.org/10.1016/S0146-6380(99)00094-7.
Smith, H.G., Blake, W.H., 2014. Sediment fingerprinting in agricultural catchments: a critical re-examination of source discrimination and data corrections. Geomorphology 204, 177–191. http://dx.doi.org/10.1016/j.geomorph.2013.08.00.
Smith, F., Freeman, K., 2006. Influence of physiology and climate on $\delta^{2}H$ of leaf wax n-alkanes from C_3 and C_4 grasses. Geochim. Cosmochim. Acta 70, 1172–1187. http://dx.doi.org/10.1016/j.gca.2005.11.006.
Thompson, J., Cassidy, R., Doody, D.G., Flynn, R., 2013. Predicting critical source areas of sediment in headwater catchments. Agric. Ecosyst. Environ. 179, 41–52. http://dx.doi.org/10.1016/j.agee.2013.07.010.
Walling, D.E., 2005. Tracing suspended sediment sources in catchments and river systems. Sci. Total Environ. 344, 159–184. http://dx.doi.org/10.1016/j.scitotenv.2005.02.011.
Walling, D.E., 2013. The evolution of sediment source fingerprinting investigations in fluvial systems. J. Soils Sediments 13, 1658–1675. http://dx.doi.org/10.1007/s11368-013-0767-2.
Wang, Y., Yang, H., Zhang, J., Xu, M., Wu, C., 2015. Biomarker and stable carbon isotopic signatures for 100–200 year sediment record in the Chaihe catchment in southwest China. Sci. Total Environ. 502, 266–275. http://dx.doi.org/10.1016/j.scitotenv.2014.09.017.
Wilkinson, S.N., Hancock, G.J., Bartley, R., Hawdon, A.A., Keen, R.J., 2013. Using sediment tracing to assess processes and spatial patterns of erosion in grazed rangelands, Burdekin River basin, Australia. Agric. Ecosyst. Environ. 180, 90–102. http://dx.doi.org/10.1016/j.agee.2012.02.002.
Withers, P.J.A., Jarvie, H.P., 2008. Delivery and cycling of phosphorous in rivers: a review. Sci. Total Environ. 400, 379–395. http://dx.doi.org/10.1016/j.scitotenv.2008.08.002.
Zech, M., Pedentchouk, N., Buggle, B., Leiber, K., Kalbitz, K., Marković, S.B., Glaser, B., 2011. Effect of leaf litter degradation and seasonality on D/H isotope ratios of *n*-alkane biomarkers. Geochim. Cosmochim. Acta 75, 4917–4928. http://dx.doi.org/10.1016/j.gca.2011.06.006.
Zhang, Z., Zhao, M., Eglinton, G., Lu, H., Huang, C.-Y., 2006. Leaf wax lipids as paleovegetational and paleoenvironmental proxies for the Chinese Loess Plateau over the last 170 kyr. Quat. Sci. Rev. 25, 575–594. http://dx.doi.org/10.1016/j.quascirev.2005.03.009.